ChemSusChem

Research Article
doi.org/10.1002/cssc.202300077

Chemistry Europe
European Chemical Societies Publishing

www.chemsuschem.org

The Role of Silicate Enrichment on the Discharge Duration of Silicon-Air Batteries

Richard Schalinski,[a] Stefan L. Schweizer,[a] and Ralf B. Wehrspohn*[a, b]

Silicon-air batteries are candidates for next generation batteries from non-critical raw materials. However, current silicon-air batteries with alkaline electrolytes suffer from premature termination of the discharge process. To understand this process, we investigated the correlation of dissolved silicon in the electrolyte and the discharge duration until passivation. The air- and Si-electrode could be excluded as the source of the voltage drop, while the concentration of silicates in the electrolyte was identified as the decisive factor. A low silicate concentration in the electrolyte was found to be crucial for a sustained discharge of silicon-air batteries with alkaline electrolytes and full consumption of the silicon electrode used in these conditions was shown.

Introduction

The ever-growing market of electronic devices demands higher storage capacities for a longer duration between charging cycles. The energy density of the most used batteries, the Li-ion batteries, is still below 250 Wh kg^{-1},[1] which motivates the development of new battery systems. In this context, metal-air and semiconductor-air batteries are particularly interesting due to their high-capacity densities.[2–10] Moreover, this kind of battery can be much lighter because of the use of air for the cathode reaction.

In 2009, Ein-Eli et al. suggested the Si-air battery (SAB) that operated with a room-temperature ionic liquid (RTIL) as the electrolyte.[11] In 2012, Zhong et al. introduced KOH as an aqueous electrolyte for SABs.[12] The first rechargeable SAB described by the group used a solid-state electrolyte that could transfer oxygen ions at 1073 K and show stable cycling at 400 Wh kg^{-1}.[9,13] The full-cell discharging and side reactions of the SAB are described in Equations (1)–(4):

$$\text{Anode (oxidation)}: \quad Si + 4OH^- \rightarrow Si(OH)_4 + 4e^- \tag{1}$$

$$\text{Cathode (reduction)}: \quad O_2 + 2H_2O + 4e^- \rightarrow 4\ OH^- \tag{2}$$

$$\text{Global reaction (red-ox)}: \quad Si + O_2 \rightarrow Si(OH)_4 \tag{3}$$

$$\text{Competing parasitic corrosion reaction}: \quad Si + 2OH^- + 2H_2O \rightarrow SiO_2(OH)_2{}^{2-} + 2H_2 \tag{4}$$

During the discharge of SAB in alkaline solutions, silicon will react with the water and hydroxide to form orthosilicic acid [Eq. (3)]. The orthosilicic acid formed diffuses from the surface into the bulk electrolyte, where it dissociates. Depending on the KOH concentration, the final product is a charged silicate $Si(OH)_{4-\beta}O_\beta^{\beta-}$ and βH^+ ions, where β is the average number of electronic charges per silicate molecule.[14–16] This diffusion process may limit the reaction rate on the silicon surface. When sufficient silicon dissolves during the reactions, the presence of different types of silicates increases the viscosity of the solution, which could hinder the diffusion of the reaction products from the electrode surface.[17] A new SAB concept used Zn^{2+} as mediator ions that transfer charge through the alkaline anolyte and acidic catholyte separated by a Zn-ion selective polyacrylonitrile membrane. This asymmetric cell enabled voltages of 2.1 V while maintaining currents of up to 0.5 mA cm^{-2}.[10] However, in all liquid electrolytes, side reactions reduce the practical capacity density to a fraction of the theoretical value, to 40–50% in RTIL electrolyte,[18] and below 5% for KOH for extended discharge.[11,17,19] Besides the capacity reduction, another challenge of these systems is the passivation of the silicon anode in aqueous electrolytes, which occurs when the reaction rate is larger than the dissolution rate of the reaction product. In-situ FTIR studies[16,20–22] found a two-step mechanism of oxide formation, where the hydrogenated surface sites are first converted into non-bridging oxygen sites (SiOH, SiO^- group), that condense and lead to a true oxide.[21] A delayed onset of oxide growth could be attributed to higher dissolution rate of the non-bridging oxygen sites at elevated temperature.[21]

Increasing this dissolution rate by adding fresh electrolyte solution to the cell at specific intervals allowed for over 1000 h of discharge.[17] Increasing the surface area of the Si electrode reduces the local reaction rate and enables the dissolution of the reaction products and, thus, the battery discharge.[12,23] However, using nanostructured electrodes with a larger surface

[a] R. Schalinski, Dr. S. L. Schweizer, Prof. Dr. R. B. Wehrspohn
Department of Physics
Martin-Luther University Halle-Wittenberg
Heinrich-Damerow-Str. 4, 06120 Halle (Germany)
E-mail: ralf.wehrspohn@physik.uni-halle.de
[b] Prof. Dr. R. B. Wehrspohn
KENTECH
21 Kentech-gil, Naju 58330, South Korea

Supporting information for this article is available on the WWW under https://doi.org/10.1002/cssc.202300077

area increases the overall corrosion rate. When in contact with high-concentration KOH electrolytes, the Si nanostructures are etched in only 5 min, leaving the plane surface and pyramidal hillocks.[24] Another way to extend the discharge duration is to influence the dissolution rate of silicates by temperature control. Continuous discharge of a planar silicon electrode in 6 mol L^{-1} KOH was only possible above a threshold temperature of 26 °C, while 20 °C was sufficient for a nanostructured Si electrode.[24] A discharge of silicon in acidic electrolytes leads to the fast growth of an oxide layer. Tao et al. demonstrated that introducing copper in the silicon anode induced defective oxide growth that exposed the electrode to the acidic electrolyte and, thus, enabled continuous cell discharge.[25]

Silicon-air batteries currently suffer from three major drawbacks: Incomplete discharge due to passivation, large overpotentials, and low efficiency due to parasitic corrosion.[26] The conversion efficiency, η(%), describes the percentage of electrochemically reacted silicon that generated a current in the outer circuit to the total amount of silicon consumed as a parameter for corrosion [Eq. (5)].

$$\eta(\%) = \frac{M_{\text{loss,tot}} - M_{\text{loss,cor}}}{M_{\text{loss,tot}}} \times 100 \quad (5)$$

Silicon-air batteries with alkaline electrolytes suffer from rapid passivation, low conversion efficiency, self-discharge, and low power density. Nevertheless, its high theoretical capacity of 3817 mAh g_{Si}^{-1} and potential of 2.09 V are environmentally and economically appealing, making this type of battery an attractive alternative to conventional batteries. To overcome the challenges of this system and enable its commercial use, a more detailed understanding of the limiting mechanisms is necessary. Thus, in this paper, we focus on the problem of the premature end of discharge of Si-air batteries in alkaline electrolytes. We have studied the effect of silicate concentration in the bulk electrolyte as a critical factor for the discharge duration of SABs at low KOH electrolyte concentrations (Figure 1). We conclude that the silicate concentration needs to be below a threshold for prolonged discharge.

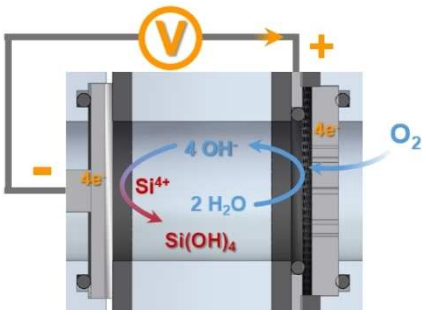

Figure 1. Schematic of the full Si-air battery test cell used in this work.

Results and Discussion

There are two main limitations to the use of Si-air batteries (SABs), corrosion, and passivation. Considering only voltage and passivation, it is beneficial to use high concentrations such as 5 mol L^{-1} KOH for long discharge duration and high-power output for SABs.[17,26] We performed galvanic discharge tests of Si-air batteries at 70 μA cm^{-2} after 30 min of open circuit voltage using KOH concentrations varying from 0.1 to 5 mol L^{-1} (Figures 2 and S1). In these experiments, we investigated the timing of the passivation event, which we determined to be the drop in cell voltage below 0.4 V. At this point, the voltage already decreases exponentially, which is due to the loss of the active surface area through progressive coverage of the electrode with oxide.[21] The local reaction rate on the exposed interface increases due to partial passivation because of the maintained constant discharge current. The total discharge duration until reaching the 0.4 V increases considerably with higher KOH concentrations from less than a minute at 0.1 mol L^{-1} to 400 h at 5 mol L^{-1} KOH (Figure 2). We also observed an increase of the conductivity and the voltage with the KOH concentration up to 5 mol L^{-1}, in agreement with the literature (Figure S1).[26,27] A KOH concentration around 5–6 mol L^{-1} is used in most studies of SABs that focus on maximum power output because the conductivity reaches its maximum in this range.[17,24,26,27] Longest discharge is observed at a 5 mol L^{-1} KOH concentration, while lower concentrations showed rapid passivation (Figure 2).[17,23] However, the highest capacity densities are reached with a significantly lower KOH concentration, under 1 mol L^{-1}.[12,28]

Besides finding the timing of the voltage drop, we also determined the concentration of dissolved silicon (in the form of silicates) at the end of each discharge test. For that, we measured the weight of the Si-electrode before and after the tests. We found that higher amounts of silicon in the electrolyte

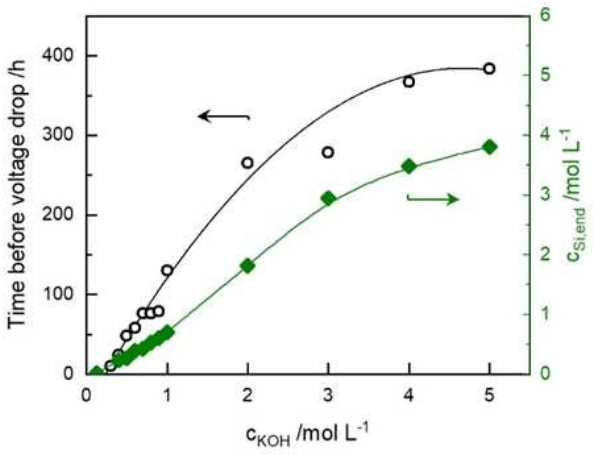

Figure 2. Galvanic discharge experiments of full Si-air-Batteries at 70 μA cm^{-2} in different KOH concentrations after 30 min at open circuit potential (OCP). The voltage drop was defined at the point in which it falls below 0.4 V. The Si-concentration is given at the end of these discharge experiments on the *y*-axis on the right side. The lines are only a guide to the eye and do not express any mathematical dependency.

solution were present for elevated concentrations of KOH (Figure 2). In these experiments, it is still a matter of debate whether more silicon dissolves because of extended discharge at higher KOH concentrations or whether the discharge time is longer due to a higher capacity for silicates.

Regarding the other main limitation of SABs, high corrosion, consider the conversion efficiency. High corrosion not only leads to inefficient use of the silicon but also to low discharge current density. The rapid etching of high surface areas like nanowires into pyramids limits the possible discharge currents.[24] In discharge tests over 24 h, we found that the efficiency is below 4% at KOH concentrations higher than 2 mol L^{-1}, while it reaches 9% at 0.5 mol L^{-1} (Figure 3). Thus, corrosion is much higher at elevated concentrations.[12,26] At low KOH concentrations, nanostructures can be used for longer discharge times by allowing low local reaction rates, which results in higher current densities.[12,23,24]

Therefore, we see two possible optimization paths to achieve extended discharge with low corrosion: 1) use a high KOH concentration and reduce the corrosion, or 2) use a low KOH concentration and increase the possible discharge duration. Here, we focus on the second path and investigate the reason for the early voltage drop at lower KOH concentrations. Therefore, we studied the different components of the battery as a possible cause for it. We started with the air-electrode because the clogging of this electrode is one of the major causes of the voltage drop in SABs with room-temperature ionic liquid as the electrolyte.[4,29]

We investigated the air-electrode in our alkaline system by monitoring the potentials of both electrodes versus the same reference while performing discharge tests. While the cell voltage follows the potential of the Si-electrode, the air-electrodes potential does not display a drop at the end of the discharge (Figure 4). SEM and EDX measurements of the used air-electrodes showed no traces of silicon oxide deposition after the tests (Figures S2, S3). According to the voltage profile (Figure 4), the potential drop occurs between the silicon and the reference electrode, located in the center of the bulk electrolyte. To explain the discharge termination after a few hours, we investigated the time-dependent mechanisms at the interface between the electrolyte and the silicon.

Upon exposure of silicon to an alkaline solution, the surfaces of {100} silicon planes are etched approximately 100 times faster than {111} planes.[30,31] Thus, pyramids containing {111} facets appear on the flat {100} silicon surface.[32] This process occurs in the first few minutes of discharge and, at low KOH concentrations, results in complete coverage of the surface with pyramids.[24,26] This shift from {100} to {111} surfaces decreases the etch rate but increases the surface by ≈73%. While that is a process that affects voltage, it occurs on a much shorter time scale than the observed sudden drop in voltage after many hours of discharge. That leaves the electrolyte as a possible source of the potential change.

Unlike non-alkaline SABs, the final product of the reaction is not silicon oxide on the cathode side. During discharge and corrosion, the silicon in alkaline SABs reacts to form silicate species, which then dissolve into the bulk electrolyte.[17] Therefore, silicates accumulate in the electrolyte solution and can change their properties over time. To investigate the effects of dissolved silicates on discharge characteristics and understand how the change in the electrolyte solution can influence the discharge, we performed galvanic discharge experiments with known quantities of pre-dissolved silicon in KOH until the voltage dropped below 0.4 V (Figure 5). We observed a clear correlation between the discharge time and the amount of dissolved silicon in the electrolyte. In the 1 mol L^{-1} KOH solution, the voltage drops earlier with increasing amounts of pre-dissolved silicon (Figure 5a). While the cell discharges continuously for 130 h in pure KOH, the voltage drops immediately when the electrolyte contains 0.75 mol L^{-1} of pre-dissolved silicon. At the end of the discharge time, the amount of consumed silicon in the electrolyte (Figure 5a, right *y*-axis)

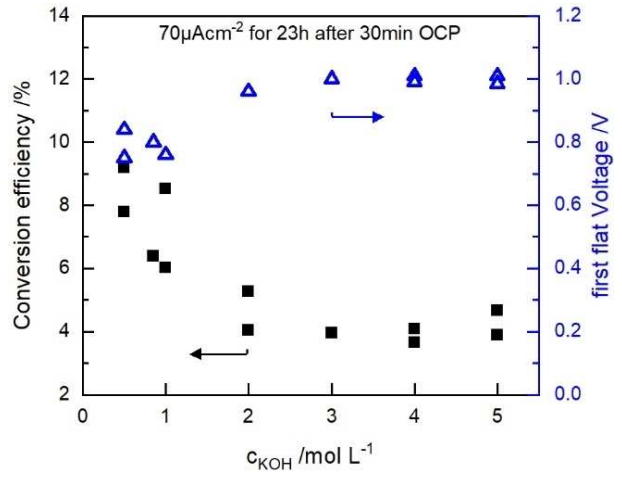

Figure 3. Conversion Efficiency (left *y*-axis) and first voltage plateau (right *y*-axis) of galvanic discharge of full SAB in different KOH solutions.

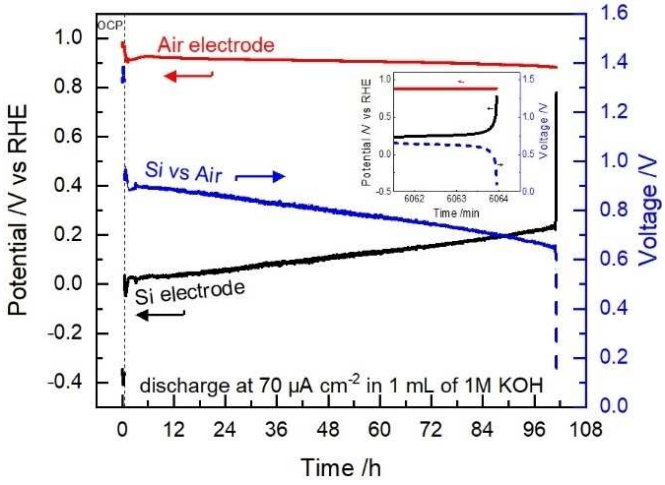

Figure 4. Galvanic discharge of a full SAB until passivation. The left axis shows the potential of the Si and air electrode compared to the RHE and the right axis shows the resulting cell voltage. The inlet zooms in on the onset of the potential drop signaling passivation.

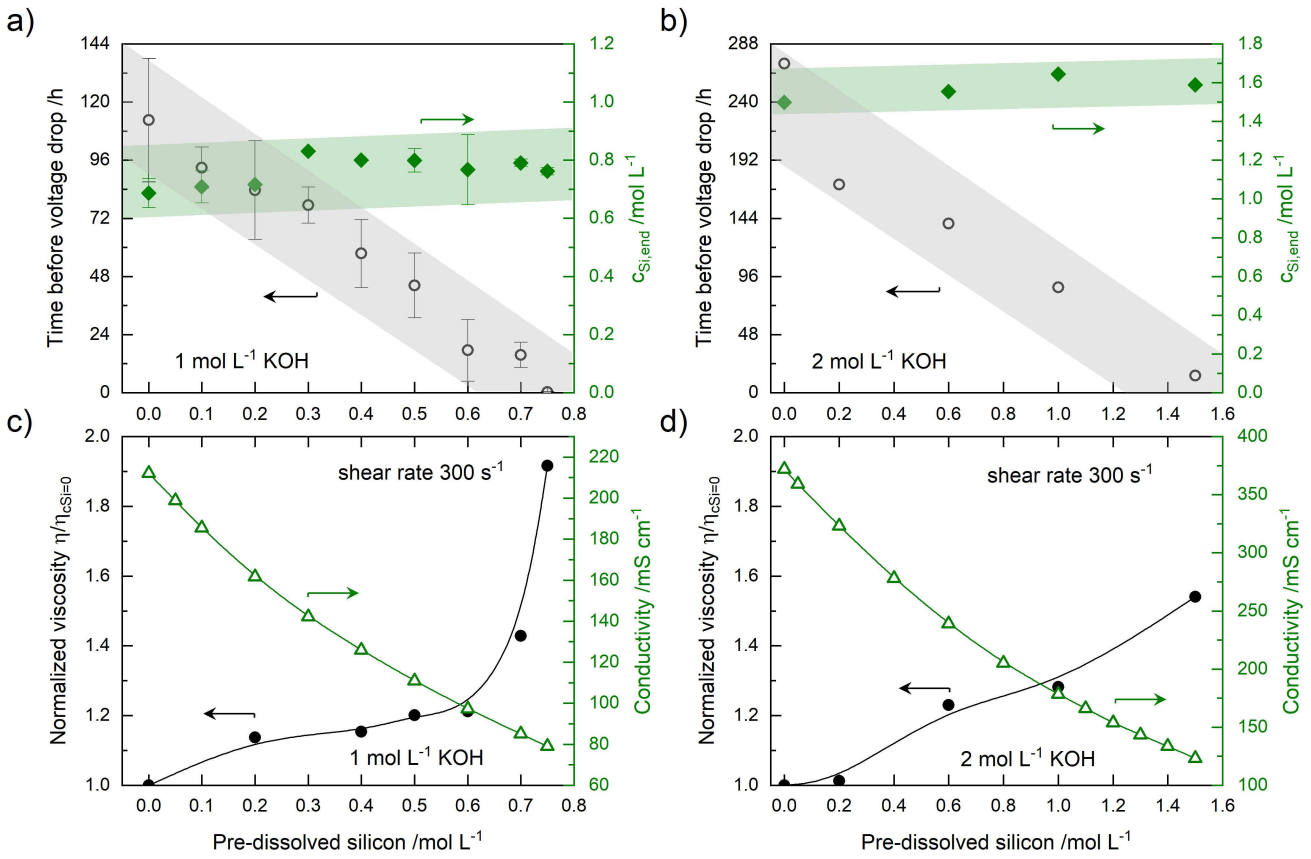

Figure 5. Discharge experiments of full silicon-air batteries at 70 μA cm^{-2} with pre-dissolved silicon containing KOH solution at concentrations of 1 mol L^{-1} (a) and 2 mol L^{-1} (b). The time before a voltage drop below 0.4 V (grey shade), indicating electrode passivation, and the Si-concentration at the end of these discharges (green shade) are given for the KOH solutions. The normalized viscosity and conductivity of the same electrolyte solutions are given for KOH concentrations of 1 mol L^{-1} (c) and 2 mol L^{-1} (d). The lines are only a guide to the eye.

indicates a concentration limit above which the dissolution rate cannot sustain the oxidation rate at 70 μA cm^{-2}. This concentration is around 0.8 mol L^{-1} of dissolved silicon for the 1 mol L^{-1} KOH solution (Figure 5a, highlighted background). A slight volume loss of the electrolyte due to evaporation during the longer discharge times explains the slightly lower final concentrations with lower pre-dissolved silicon. The same trend of shorter discharge times at a higher pre-dissolved silicon concentration is present for the 2 mol L^{-1} KOH solution, where the limit of dissolved silicon concentration is around 1.6 mol L^{-1} (Figure 5b). While a discharge of 271 h was possible without pre-dissolved silicon, the discharge duration decreased to only 14 h at a concentration of 1.5 mol L^{-1}, indicating that the dissolved silicon is close to its limit. Thus, the silicate concentration in the bulk electrolyte affects surface passivation. The higher the dissolved Si concentration in the KOH solution, the shorter the discharge times. Larger oligomers and cyclic silicate species are present in alkaline SABs.[17] In the literature, the lower conductivity is attributed to an increase in viscosity due to the gelation of the silicates.[17] In our experiments, the viscosity increases exponentially for concentrations above 0.6 mol L^{-1} of silicon in 1 mol L^{-1} KOH solution (Figure 5c) while the conductivity decreases steadily. That could be because the charge-carrying ion with the highest mobility is OH^-, which remains unaffected by the enhanced viscosity due to the reverse Grotthuss mechanism.[33–35] The sudden change in viscosity coincides with the onset of passivation of the silicon surface. The increase in viscosity between the pure 1 mol L^{-1} KOH and the one containing 0.75 mol L^{-1} of pre-dissolved silicon (Figure 5c) is equivalent to the viscosity increase between 1 and 6 mol L^{-1} KOH.[36] We expect a much longer discharge time despite the high viscosity at this high KOH concentration of 6 mol L^{-1}. Therefore, our experiments show neither conductivity nor viscosity to indicate the voltage drop. As observed for the 1 mol L^{-1} KOH solution, the viscosity of the 2 mol L^{-1} KOH solution also increases with the silicon content. However, there is no abrupt change in the slope of the viscosity curve in the range tested (Figure 5d), which could be due to the maximum silicon concentration of 1.5 mol L^{-1} used. In analogy to the experiment with 1 mol L^{-1} KOH, this change in viscosity might be observed only above the threshold concentration of dissolved silicon of 1.6 mol L^{-1} (Figure 5b, green shade). Thus, the concentration of silicate species in the electrolyte correlates with the discharge duration.

It is accepted in the literature that passivation of the silicon surface occurs when the production rate of silicates exceeds the dissolution rate in the bulk electrolyte.[12,17,23] To investigate this, we analyzed the reaction rates to determine the sustainable

dissolution rate. If the dissolution rate changes with the silicon concentration, we should then be able to see a dependency on the possible discharge time with different current densities. Therefore, we discharged at different current densities and measured the discharge time in 1 mol L^{-1} + 0.7 mol L^{-1} pre-dissolved silicon, close to the maximum concentration determined for 70 μA cm^{-2} (Figure 6). Measuring the weight of the consumed Si-electrode after the test finished revealed that, with 0.8 mol L^{-1} of dissolved Si in the electrolyte, a current of 70 μA cm^{-2} leads to passivation. This current density equals an electrochemical reaction rate of 0.0218 nm s^{-1}. At the onset of passivation, we can determine the silicate dissolution rate as equal to the silicate production rate. Accordingly, discharging in a 1 mol L^{-1} KOH solution with a current density of 50 μA cm^{-2} passivated the silicon surface at a concentration of 0.92 mol L^{-1}. We identified a dependency of the discharge time on the current density and, therefore, on the reaction rate. Our experiment shows that above 30 μA cm^{-2} with higher reaction rates, less silicon can be dissolved in the electrolyte before the dissolution rate drops and the surface passivates (Figure 6, right axis). That extends the possible discharge time for lower current densities.

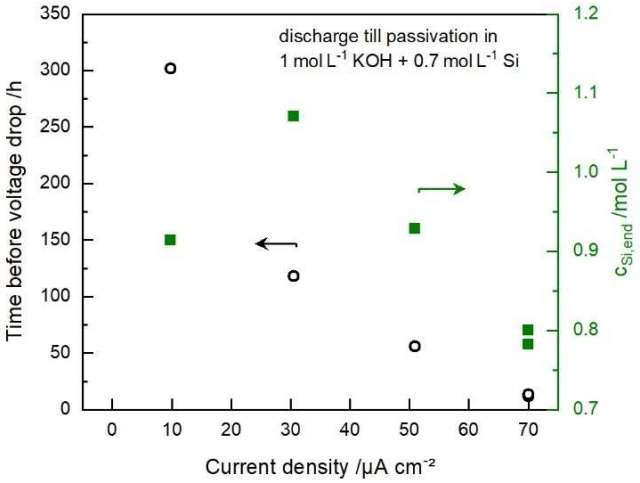

Figure 6. Galvanostatic discharge at different currents in 1 mol L^{-1} KOH containing 0.7 mol L^{-1} of pre-dissolved silicon. Duration before passivation (lefy *y*-axis) and the corresponding concentration of dissolved silicon at the end (right *y*-axis).

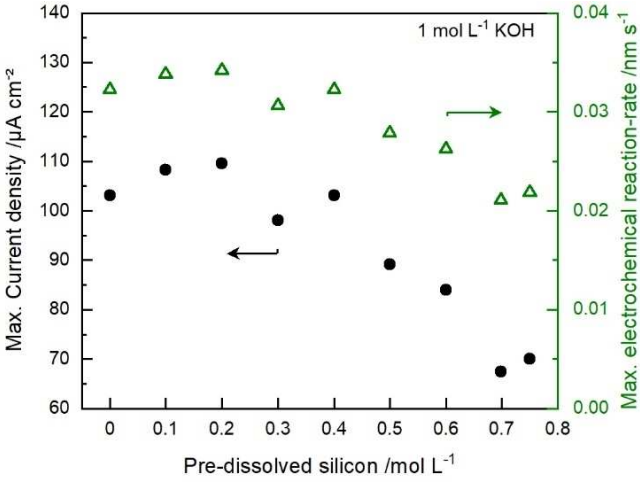

Figure 7. Maximum possible discharge current (lefy *y*-axis) and corresponding maximum reaction rate (lefy y-right axis) from galvanostatic step polarization experiments of full SAB with 1 mol L^{-1} KOH containing different amounts of pre-dissolved silicon with 5 min hold times.

We also observed this relation between the maximum discharge rate and concentration of dissolved silicon in the galvanic step polarization experiments (Figure 7). We measured the voltage of full SABs with 1 mol L^{-1} KOH with different amounts of pre-dissolved silicon while controlling the current in a range from 65 to 140 μA cm^{-2} in steps of 5 μA cm^{-2}, while holding it for 5 min followed by 1 min of OCP in between. A discharge duration of 5 min is sufficient to exclude passivation of the surface, as this takes place in periods of less than one minute (Figure 4 inlet). The maximum current density for discharge is around 110 μA cm^{-2} for the pure 1 mol L^{-1} KOH electrolyte and falls below 70 μA cm^{-2} with 0.7 mol L^{-1} of pre-dissolved silicon. From this, we can calculate the maximum electrochemical reaction rate above which the surface passivates, assuming that the parasitic reaction rate stays constant (Figure 7, right axis). The measurements also show that the dissolution rate of the silicates and, thus, the maximum discharge rate is impacted even at low silicate concentrations. The reduced reaction rate before large oligomers condensates hints at a diffusion-limited process.

The silicon can be consumed without passivation when the Si concentration stays suffiently low. In other words, as long as the dissolution of the silicates from the surface is fast enough, no passivation layer leads to a potential drop. Indeed, a full 3 mm thick Si-electrode can be discharged fully in over 1100 h, when the electrolyte refills every four hours.[17] In our experiments, we have chosen an enlarged reservoir of 300 mL for the electrolyte instead of a pump system to exclude flow-related effects without changing the distance between the electrodes (Figure 8). This prevents sluggish layers from detaching from the surface during the fluid exchange. Using an excess of electrolyte, we were able to keep the silicate concentration below the threshold concentration and consume the entire Si-electrode even at low KOH concentrations over 440 h of discharge (Figure 8). Thus, our experiments show that the silicate concentration in the bulk electrolyte determines the moment of passivation. The silicate concentration must be kept low, to extend the discharge duration. Passivation indeed happens when the production rate of silicates exceeds their dissolution rate.

Conclusions

Current silicon-air batteries with alkaline electrolytes suffer from premature termination of the discharge process. To understand the process of premature passivation, we investigated the correlation between dissolved silicon in the electrolyte and the discharge duration until passivation. While the use of electro-

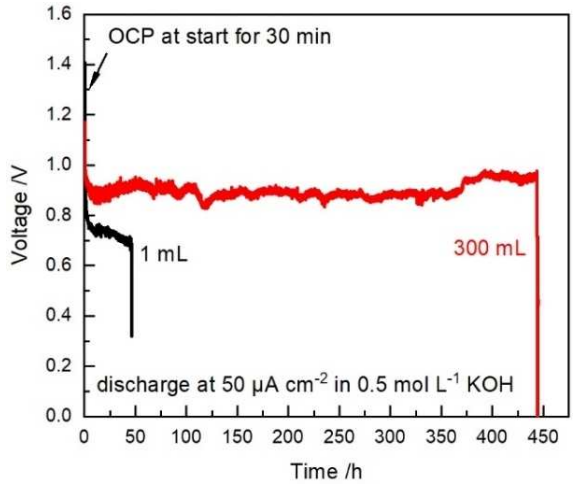

Figure 8. Voltage profile of the discharge of full SABs at 50 $\mu A\,cm^{-2}$ in 0.5 $mol\,L^{-1}$ KOH with 1 mL and 300 mL. The potential drop with the 300 mL electrolyte is due to the full dissolution of the silicon electrode.

lytes with high KOH concentrations up to 5 $mol\,L^{-1}$ still allows for long discharge times, they suffer from severe corrosion, which prevents the use of high surface area materials. The use of low KOH concentrations in silicon-air batteries reduces corrosion, but the discharge is limited by rapid passivation.

The silicate concentration of the bulk electrolyte, which builds up over time due to corrosion and discharge reactions, leads to the premature passivation of the silicon electrode. More precisely, the reduction of the reaction product diffusion from the surface into the bulk electrolyte leads to oxide formation. Here, we identified neither conductivity nor viscosity of the electrolyte as indicators for the voltage drop. Therefore, our results suggest that the dissolution rate is simply limited by diffusion due to the concentration gradient of the silicates from the surface to the bulk electrolyte.

For a 1 $mol\,L^{-1}$ KOH electrolyte solution, we have determined that the critical concentration of dissolved silicon in the bulk electrolyte is 0.8 $mol\,L^{-1}$ above which the silicon surface passivates at a discharge current of 70 $\mu A\,cm^{-2}$. The maximum possible discharge current is limited by the amount of dissolved silicon in the electrolyte, with even small amounts causing a reduction of the current. If the silicon concentration is kept sufficiently low by using large electrolyte volumes, the silicon electrodes can dissolve completely, even at KOH concentrations as low as 0.5 $mol\,L^{-1}$ over 440 h.

To prolong the discharge effectively, we propose two possible pathways: reducing the rate of silicate generation or enhancing the diffusion by decreasing the concentration in the electrolyte.

Decreasing the parasitic corrosion reaction would reduce the number of silicates generated and, thus, the concentration in the electrolyte. To keep silicate concentration to a minimum, we propose targeted precipitation that does not block any paths in the air electrode. Furthermore, additives could support the diffusion of the silicates away from the surface. Further research is needed to enable enhanced discharge of SABs.

Experimental Section

Chemicals and materials

N-type Si (100) wafers (Silicon Materials, 1–10 Ω cm, phosphor-doped) with a thickness of 525 +/− 25 µm were laser cut, cleaned with isopropanol, and then Piranha etching solution (3 parts 98% H_2SO_4 to 1 part 30% H_2O_2) for 10 min and then thoroughly rinsed with deionized water. The native oxide film was removed with 5% HF before assembly in the test cell.

Preparation of the electrolytes

Solutions with KOH concentrations from 0.1 to 5 $mol\,L^{-1}$ were prepared from KOH pellets (> 85 %, Sigma Aldrich) and used as the electrolyte. For tests with pre-dissolved silicon, the n-type Si-wafers were dissolved in 2 $mol\,L^{-1}$ KOH under ultrasound and further diluted to the necessary concentrations. The solution's conductivity was measured with a Tetracon 325 (WTW Inolab Cond720) conductometer.

Electrochemical testing

A commercial air electrode with manganese mixed oxide catalyst on a nickel mesh (Gaskatel, Germany) was used as the cathode. The test cell is made of PVC with EPDM fittings and stainless-steel current collectors. The active area of the electrodes in contact with the electrolyte is 10 mm in diameter. If not noted otherwise, tests were conducted at 25 °C with an electrolyte volume of 1 mL. Galvanic discharge measurements were performed in 2-electrode configuration with the battery cycler BTS3000 (Neware). The measurements in 3-electrode configuration were performed with the potentiostat VIONIC (Metrohm) in the same cell setup as the 2-electrode configuration. A reversible hydrogen electrode was used as a reference electrode in between the silicon and the air-electrode. The full cells were kept at open circuit potential for 30 min after assembly and then discharged at 70 $\mu A\,cm^{-2}$ for various times, followed by 30 min at OCP. As the criteria for the passivation event, a voltage drop below 0.4 V was defined. The weight of the Silicon was measured before and after discharge tests using a high precision scale to determine the capacity density and the dissolved silicon concentration based on the initial electrolyte volume. Galvanic step polarization curves were measured in 2-electrode configuration starting after 30 min at OCP from 65 to 140 $\mu A\,cm^{-2}$ in steps of 5 $\mu A\,cm^{-2}$ while holding the current for 5 min followed by 1 min of OCP in between to guarantee the dissolution of products on the surface. The maximum current density was then determined as the current where a full 5 min discharge was still possible.

Mechanical testing

Dynamic viscosity measurements were performed at room temperature using an Anton Paar MCR501 Twin-Drive rheometer with stainless steel plates at a shear rate of 300 s^{-1} and normalized with the viscosity of the respective pure KOH solution without pre-dissolved silicon.

Acknowledgements

The authors acknowledge the fruitful discussions with Dr. Juliana Martins de Souza e Silva. Open Access funding enabled and organized by Projekt DEAL.

Conflict of Interests

The authors declare no conflict of interest.

Data Availability Statement

The data that support the findings of this study are available from the corresponding author upon reasonable request.

Keywords: Silicon-Air Batteries · Passivation · Alkaline media · Electrochemistry · Electrolyte

[1] P. Albertus, S. Babinec, S. Litzelman, A. Newman, *Nat. Energy* **2018**, *3*, 16–21.
[2] G. Cohn, A. Altberg, D. D. MacDonald, Y. Ein-Eli, *Electrochim. Acta* **2011**, *58*, 161–164.
[3] G. Cohn, R. A. Eichel, Y. Ein-Eli, *Phys. Chem. Chem. Phys.* **2013**, *15*, 3256.
[4] G. Cohn, Y. Ein-Eli, *J. Power Sources* **2010**, *195*, 4963–4970.
[5] J. D. Ocon, J. W. Kim, G. H. A. Abrenica, J. K. Lee, J. Lee, *Phys. Chem. Chem. Phys.* **2014**, *16*, 22487–22494.
[6] J. D. Ocon, G. H. A. Abrenica, J. Lee, *ChemElectroChem* **2016**, *3*, 242–246.
[7] H. Weinrich, Y. E. Durmus, H. Tempel, H. Kungl, R. A. Eichel, *Materials* **2019**, *12*, 2134.
[8] A. Inoishi, T. Sakai, Y. W. Ju, S. Ida, T. Ishihara, *J. Mater. Chem. A* **2013**, *1*, 15212–15215.
[9] A. Inoishi, H.-H. Kim, T. Sakai, Y.-W. Ju, S. Ida, T. Ishihara, *ChemSusChem* **2015**, *8*, 1264–1269.
[10] C. Lin, S.-H. Kim, Q. Xu, D.-H. Kim, G. Ali, S. S. Shinde, S. Yang, Y. Yang, X. Li, Z. Jiang, J.-H. Lee, *Matter* **2021**, *4*, 1287–1304.
[11] G. Cohn, D. Starosvetsky, R. Hagiwara, D. D. Macdonald, Y. Ein-Eli, *Electrochem. Commun.* **2009**, *11*, 1916–1918.
[12] X. Zhong, H. Zhang, Y. Liu, J. Bai, L. Liao, Y. Huang, X. Duan, *ChemSusChem* **2012**, *5*, 177–180.
[13] A. Inoishi, T. Sakai, Y.-W. Ju, S. Ida, T. Ishihara, *J. Mater. Chem. A* **2013**, *1*, 15212.
[14] H. Seidel, L. Csepregi, A. Heuberger, H. Baumgärtel, *J. Electrochem. Soc.* **1990**, *137*, 3626.
[15] E. D. Palik, H. F. Gra, P. B. Klein, *J. Electrochem. Soc.* **1983**, *130*, 956.
[16] D. Lapadatu, R. Puers, *Sens. Actuators A Phys.* **1997**, *60*, 191–196.
[17] Y. E. Durmus, Ö. Aslanbas, S. Kayser, H. Tempel, F. Hausen, L. G. J. G. J. de Haart, J. Granwehr, Y. Ein-Eli, R.-A. A. Eichel, H. Kungl, *Electrochim. Acta* **2017**, *225*, 215–224.
[18] Y. E. Durmus, S. Jakobi, T. Beuse, Ö. Aslanbas, H. Tempel, F. Hausen, L. G. J. de Haart, Y. Ein-Eli, R.-A. Eichel, H. Kungl, *J. Electrochem. Soc.* **2017**, *164*, A2310–A2320.
[19] D. Chen, Y. Li, X. Zhang, S. Hu, Y. Yu, *J. Ind. Eng. Chem.* **2022**, *112*, 271–278.
[20] X. H. Xia, J. J. Kelly, *Phys. Chem. Chem. Phys.* **2001**, *3*, 5304–5310.
[21] H. G. G. Philipsen, F. Ozanam, P. Allongue, J. J. Kelly, J.-N. Chazalviel, *J. Electrochem. Soc.* **2016**, *163*, H327–H338.
[22] H. G. G. Philipsen, J. J. Kelly, *Passivation of (100) and (111) Silicon in KOH Solution*, Elsevier B. V., **2006**.
[23] D. W. Park, S. Kim, J. D. Ocon, G. H. A. Abrenica, J. K. Lee, J. Lee, *ACS Appl. Mater. Interfaces* **2015**, *7*, 3126–3132.
[24] S. Sarwar, M. Kim, G. Baek, I. Oh, H. Lee, *Bull. Korean Chem. Soc.* **2016**, *37*, 997–1003.
[25] Y. Tao, Q. Zhou, C. Cai, C. Song, H. Li, X. Huang, L. Yang, W. Huang, S. Li, *Energy Environ. Sci.* **2021**, *14*, 6672–6677.
[26] Y. E. Durmus, S. S. Montiel Guerrero, Ö. Aslanbas, H. Tempel, F. Hausen, L. G. J. de Haart, Y. Ein-Eli, R. A. Eichel, H. Kungl, *Electrochim. Acta* **2018**, *265*, 292–302.
[27] R. J. Gilliam, J. W. Graydon, D. W. Kirk, S. J. Thorpe, *Int. J. Hydrogen Energy* **2007**, *32*, 359–364.
[28] A. Garamoun, M. B. Schubert, J. H. Werner, *ChemSusChem* **2014**, *7*, 3272–3274.
[29] P. Jakes, G. Cohn, Y. Ein-Eli, F. Scheiba, H. Ehrenberg, R. A. Eichel, *ChemSusChem* **2012**, *5*, 2278–2285.
[30] E. D. Palik, V. M. Bermudez, O. J. Glembocki, *J. Electrochem. Soc.* **1985**, *132*, 871.
[31] J. W. Faust, E. D. Palik, *J. Electrochem. Soc.* **1983**, *130*, 1413.
[32] P. Raisch, W. Haiss, R. Nichols, D. Schiffrin, *Electrochim. Acta* **2000**, *45*, 4635–4643.
[33] M. E. Tuckerman, D. Marx, M. Parrinello, *Nature* **2002**, *417*, 925–929.
[34] C. J. T. yon Grotthuss, *Ann. Chim.* **1806**, pp. 54–73.
[35] N. Agmon, *Chem. Phys. Lett.* **1995**, *244*, 456–462.
[36] P. M. Sipos, G. Hefter, P. M. May, *J. Chem. Eng. Data* **2000**, *45*, 613–617.

Manuscript received: January 17, 2023
Revised manuscript received: March 30, 2023
Accepted manuscript online: April 14, 2023
Version of record online: June 28, 2023